Preparation and Adsorption Properties of Corncob-Derived Activated Carbon with High Surface Area

Y. X. Wang, B. S. Liu,* and C. Zheng

Department of Chemistry, School of Science, Tianjin University, Tianjin 300072, China

Corncob, a widespread and inexpensive natural resource in China, was used to prepare activated carbon (AC) by chemical activation with potassium hydroxide (KOH). The adsorption equilibrium and kinetics of H_2, CH_4, and CO_2 on AC were investigated at different temperatures. Adsorption isotherms of H_2, CH_4, and CO_2 were correlated with the Langmuir and Freundich equations, and the heat of adsorption was determined. It was revealed that the Freundich adsorption equation was more apt to describe the adsorption procedure of H_2, CH_4, and CO_2 compared to the Langmuir equation. Two simplified kinetic models including pseudo-first-order and -second-order equations were used to evaluate the adsorption processes. The results indicated that the adsorption of H_2, CH_4, and CO_2 could be described properly by a pseudo-second-order equation. The kinetic parameters of this model were calculated and discussed.

Introduction

Environmental friendly energy sources can protect the world from severe pollution emanating from the burning of fossil fuel and can also reduce the reliance on petroleum supply. Both H_2 and CH_4 are renewable clean energy sources, but the use of a storage technology with low cost and high energy density is of critical importance for natural gas vehicles. Adsorption can enhance the storage of gaseous fuels. Therefore, studies on the sorption behavior of hydrogen and methane on different materials have attracted considerable attention.[1] Emissions from the combustion of fossil fuels are contributing to an increase in the concentration of CO_2 in the atmosphere. Both CO_2 and CH_4 are green house gas and can result in global climate change. Consequently, extensive effort has been undertaken recently for the removal of CO_2 from industrial flue gas as a potential means of mitigating CO_2 emissions in the world. As a more promising method for CO_2 capture, adsorption offers potential energy savings, especially with respect to compression costs.[2]

Physical adsorption is widely used for the separation and purification of gases.[3] Biogas mainly consists of methane and carbon dioxide. In Japan, biogas generated in a sewage treatment plant is desulfurized and stored in gas holders for use as a boiler fuel and/or for power generation. The development of such a system of adsorption-based processes requires basic adsorption equilibrium data that are necessary to measure precise isotherms for pure substances across a wide range of temperatures. Recently, intensive work was performed to identify adsorbents under different operating conditions, including high and normal pressure adsorption. Though the gas adsorption amount was high under high pressure, it is more convenient and cost-effective to measure basic data correlated with adsorption capacity of adsorbents at atmospheric pressure.

The cost of the adsorbent material is a very important criterion for its industrial application. Activated carbon (AC) is a valuable adsorbent due to its porous structure and low cost. Corncob as a biomass and agricultural waste is an attractive candidate. Usage of these biomass wastes as a raw material for production of AC is a highly beneficial undertaking for obvious reasons. El-Hendawy et al. prepared AC from corncobs by physical and chemical activation and measured the adsorption capacities of iodine, phenol, and methylene blue over AC.[4,5] The influence of HNO_3 oxidation on the porosity and adsorptive properties of corncob-based ACs was also investigated;[5,6] however, the specific surface area of the obtained ACs was low (<1000 $m^2 \cdot g^{-1}$). Amphol et al. prepared micromesoporous ACs from corncobs by CO_2 activation and investigated the adsorption equilibrium of monoethylene glycol on the ACs.[7,8] According to the report of Cao et al.,[9] high surface area-activated carbons (HSAAC) can be prepared from corncobs by KOH activation. Tseng et al. prepared HSAAC by KOH activation and studied only the adsorption kinetics of methylene blue, 2,4-dichlorophenol, phenol, etc., on the ACs.[10,11]

The gas sorption capacity of AC generally increases with specific surface area. It is therefore desirable to prepare HSAAC. It is reported that an adiabatic expansion process during thermal degradation of the material before carbonization was favorable for the creation of microporous AC,[12] and KOH activation is an adequate method for the preparation of HSAAC.[9,10] To the best of our knowledge, the combination of expansion pretreatment of corncob and KOH activation for the production of HSAAC has not been reported yet. Though adsorption performances in the liquid phase have been surveyed for corncob-based ACs,[10,11] its application on gas adsorption at low temperature has scarcely been reported.

In the present work, the corncob was first pretreated by the procedure of adiabatic expansion. The aforementioned materials were then carbonized in N_2 and activated with KOH to generate HSAAC in order to probe its potential application for the storage of H_2, CH_4, and CO_2 at low temperature.

Experimental Section

Preparation of AC. Dry corncobs from northeast China were collected and crushed to a particles size of (0.5 to 1) cm. About 70 g of corncob was placed in a horizontal airtight reactor heated externally at a definite rate. When the pressure in the reactor reached 1 MPa, the valve was opened immediately to lead to adiabatic expansion and sudden cooling. The pretreated sample

* To whom correspondence should be addressed. E-mail: bingsiliu@tju.edu.cn.

10.1021/je1002913
Published on Web 09/13/2010

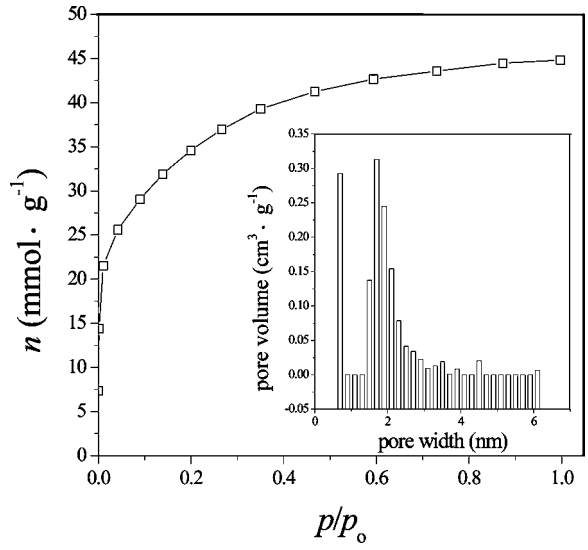

Figure 1. N_2 adsorption isotherms over AC at 77 K (inset is pore size distribution).

was heated to 450 °C at a rate of 5 °C·min^{-1} and then held at 450 °C in N_2 for 0.5 h. The carbonized sample was ground into particles of less than 0.85 mm in diameter and then soaked in saturated KOH solution (the weight ratio of KOH/char is 4:1) at 80 °C for 24 h. After soaking, the sample was dried in a vacuum at 120 °C for 24 h. Dry samples were activated at 800 °C for 1 h in nitrogen (40 mL·min^{-1}) at a rate of 10 °C·min^{-1}. The products were washed with deionized water until the pH > 6, and hence AC was obtained.

Physical Properties of AC. The AC were crushed and sieved to small grains with a diameter less than 0.25 mm and dried at 120 °C for 24 h. The characterization of AC was conducted using a nitrogen adsorption instrument at 77 K. The specific surface area (S_{BET}) was evaluated according to the BET theory,[13] and the total pore volume (V_T) was estimated by the amount adsorbed at $p/p^0 = 0.95$, and that of micropores was determined by the Dubinin−Radushkevich (DR) equation. The pore size distribution of the sample was calculated based on the simplified local density function model of the isotherm[14] and a discrete distribution function of pore sizes[15] in the range of (0.7 to 6.1) nm. The microstructure of the obtained HSAACs was observed by means of scanning electron microscopy with a field emission gun (FEI, Nanosem 430), and the elemental composition was analyzed by energy-dispersive X-ray spectrometry (EDX).

Adsorption of CH_4, H_2, and CO_2 at Low Temperature. The AC was further levigated into grains with a diameter less than 0.25 mm. Adsorption isotherms of H_2, CH_4, and CO_2 on AC were collected in a typical volumetric system, calibrated with helium. The apparatus was made of Pyrex glass and equipped with grease-free valves. An initial sample was degassed under vacuum at 473 K for 2 h. The equilibrium pressures were measured by a pressure transducer covering a range from (0.01

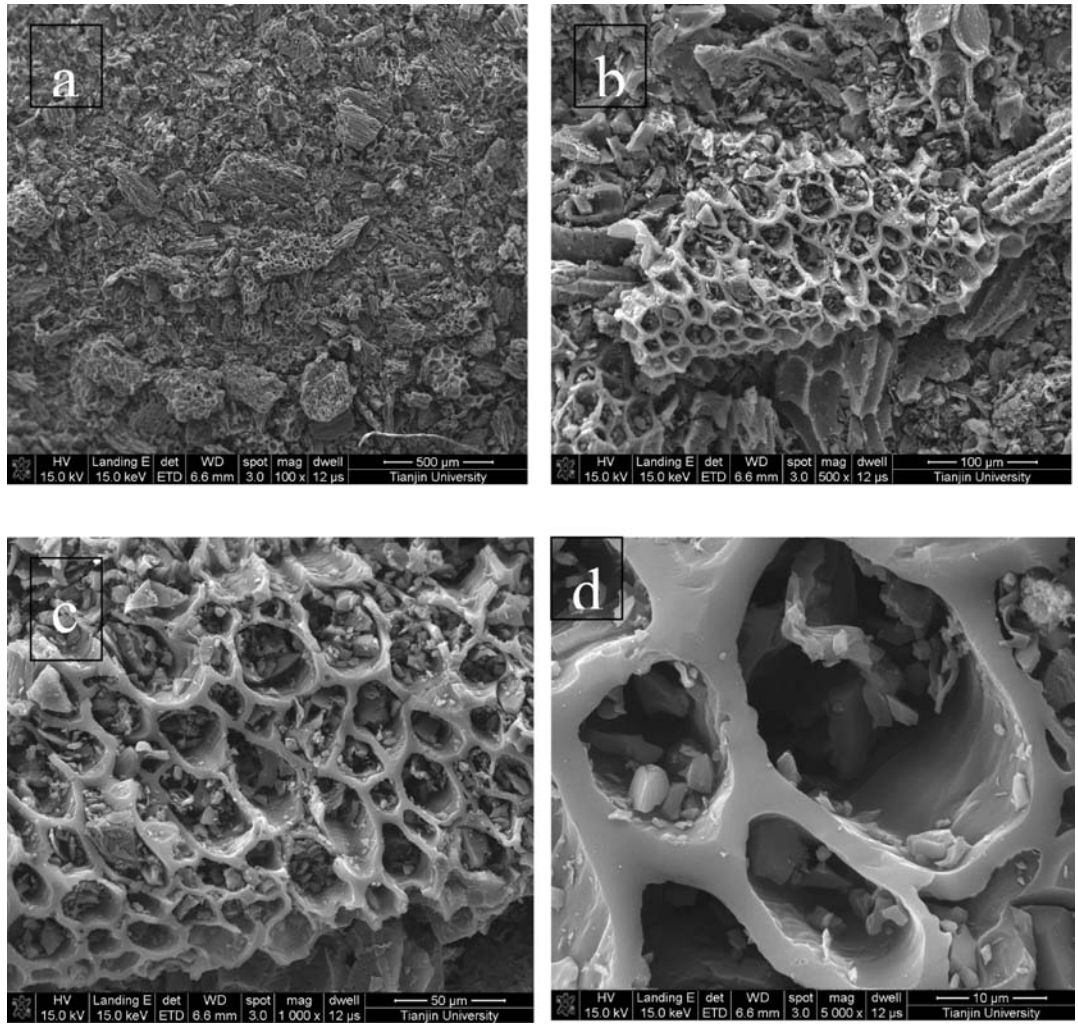

Figure 2. SEM photographs of the corncob-based HSAACs: (a) scale 500 μm, (b) scale 100 μm, (c) scale 50 μm, (d) scale 10 μm.

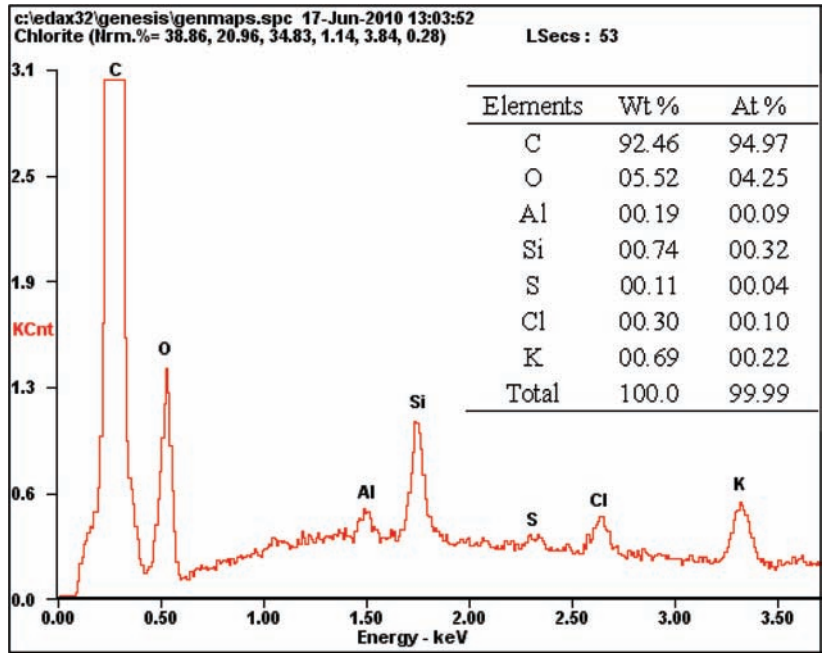

Figure 3. EDX analysis of the corncob-based HSAACs.

to 101) kPa. The adsorption of H_2, CH_4, and CO_2 at a given temperature was investigated. The temperature in the sample bath was monitored constantly with a catathermometer, and the mean deviation of temperature was less than ±0.5 K during the whole experiment. Corresponding temperatures [(77, 176, 195, 213, 226, 273, and 301) K] were maintained using liquid nitrogen (LN), a mixture of LN and n-butanol, an ice−water bath, and room temperature. Kinetic data were measured under an initial pressure of 101 kPa.

Results and Comments

Physical Properties of Corncob-Derived AC. N_2 adsorption isotherms and the pore size distribution of AC are shown in Figure 1. As expected, a character of Type-I adsorption isotherm indicated that the physical adsorption of N_2 mainly occurred on the microporous structure. The S_{BET} and V_T are 2789 $m^2 \cdot g^{-1}$ and 1.55 $cm^3 \cdot g^{-1}$, respectively; the micropore volume is 1.37 $cm^3 \cdot g^{-1}$, significantly higher than the results (S_{BET} and V_T are 2402 $m^2 \cdot g^{-1}$ and 1.29 $cm^3 \cdot g^{-1}$, V_{mic} =1.09 $cm^3 \cdot g^{-1}$) reported by Tseng et al.[10] The different results were due to the variable conditions, such as N_2 flow rate and carbonization time, except that the corncob was pretreated by adiabatic expansion. The pore size distribution reveals that the pore size is concentrated on 1.7 nm. The SEM photographs of corncob-based HSAACs with different magnification are shown in Figure 2. The honeycomb shaped holes are well arranged and regular. The walls of these holes were thick and smooth with clear angle lines. It is interesting to note that there are a large amount of irregular granules dispersed in the holes of HSAACs. According to a report in the literature,[10] the large holes originated from the corncob precursors, which are not detectable by the N_2 adsorption technique of the BET method. Therefore, the high S_{BET} and V_T obtained may originate from the existence of these irregular granules, which is favorable for the adsorption of small molecule gases at low temperature. The EDX analysis of the HSAACs (Figure 3) revealed the existence of oxygen, silicon, potassium, chlorinum, aluminum, and sulfur in addition to large amounts of carbon species.

Adsorption Performance of CH_4, H_2, and CO_2 onto Corncob-Derived AC. As shown in Figure 4, the adsorption isotherms of H_2, CH_4, and CO_2 on AC at different temperatures presented characteristics of Type-I. The adsorption amount increases rapidly with increasing pressure in the low pressure range, indicating the strong interaction of H_2, CH_4, and CO_2 with AC. The adsorption amount decreased with the increase of temperature at the same pressure due to the exothermic feature of gas adsorption (Figure 4b,c). The adsorption of gas at low temperature was more favorable.

Under the condition of 101 kPa, the adsorption amount of H_2 reached 12.76 $mmol \cdot g^{-1}$ at 77 K (Table 1), significantly higher than those reported in the literature.[16−21] This is because AC has a high S_{BET} (2789 $m^2 \cdot g^{-1}$) and large V_T (1.55 $cm^3 \cdot g^{-1}$), which benefit H_2 adsorption. As listed in Table 1, the adsorption amount of CO_2 on AC was higher than those on the other adsorbents[22−27] under similar conditions. The adsorption amount of CH_4 on other adsorbents under similar conditions (101 kPa, (176 to 213) K) has not been reported. The ACs prepared here from corncob exhibited high adsorption capacities for H_2, CH_4, and CO_2, which is a promising adsorption material for gas storage.

An adsorption isotherm can describe in principle the interaction of adsorbates with adsorbents. According to the assumption of Langmuir (L), gas molecules are adsorbed onto the surface containing a finite number of adsorption sites in a monolayer without interaction between adsorbates while Freundlich (F) developed the L isotherm model and assumed heterogeneous surface energies, in which the energy term varies as a function of the surface coverage.[28] The Langmuir and Freundlich isotherm equations are given, respectively, as follows:

$$\frac{1}{n} = \frac{1}{n_m} + \frac{1}{bpn_m} \quad (1)$$

$$n = kp^{1/q} \quad (2)$$

where n is the equilibrium adsorption amount ($mmol \cdot g^{-1}$), p is the equilibrium pressure (kPa), n_m ($mmol \cdot g^{-1}$) and b (kPa^{-1}) are the Langmuir constants, and k ($mmol \cdot g^{-1} \cdot (kPa)^{-1/q}$) and q are the Freundlich constants. We used the L and F models to correlate our experimental equilibrium data, and the results are listed in Table 2. The applicability of the isotherm equation is

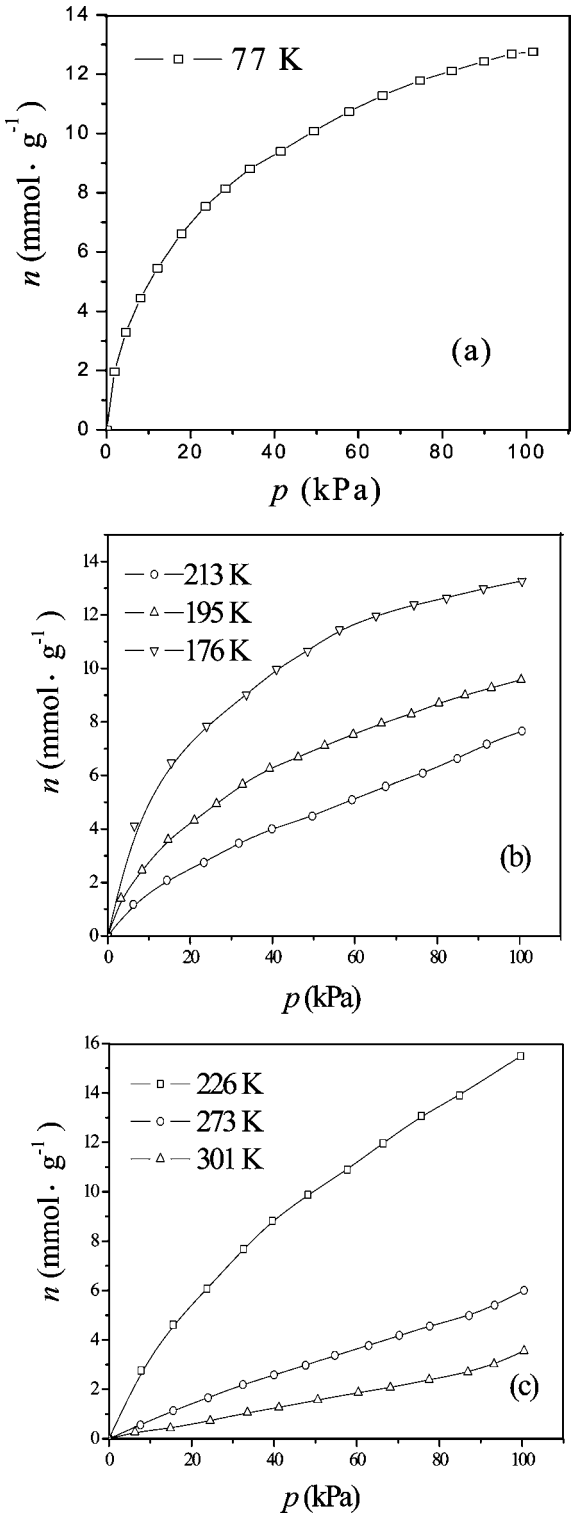

Figure 4. Adsorption isotherms of (a) H_2, (b) CH_4, and (c) CO_2 at different temperatures.

compared by judging the coefficients of determination, R^2, and the average deviation ΔN was utilized to compare the correlation results with experimental data:

$$\Delta N = \frac{1}{k}\sum\left|\frac{N_{exp} - N_{cal}}{N_{exp}}\right| \quad (3)$$

where N_{exp} and N_{cal} represent the experimental and calculated adsorption amount and k is the number of data points.

Table 1. Adsorption of H_2 and CO_2 over Different Adsorbents at 0.1 MPa[a]

adsorbates	adsorbents	T (K)	n_e (mmol·g^{-1})	ref
H_2	AC	77	12.76	this work
H_2	ZSM-5	77	3.5	16
H_2	MWCNT	77	0.97	17
H_2	N-enriched carbon	77	0.25	17
H_2	MOF-5	77	6.5	18
H_2	AC	77	9.0	19
H_2	AC fiber	77	11.15	20
H_2	SWNT	77	3.5	21
CO_2	AC	301	3.56	this work
CO_2	AC	273	6.00	this work
CO_2	N-enriched carbons	298	2.25	22
CO_2	AC	298	2.18	23
CO_2	AC	298	1.66	24
CO_2	activated anthracites	303	1.49	25
CO_2	natural zeolites	300	2.60	26
CO_2	AC fiber-resin composites	298	2.90	27
CO_2	AC fiber-resin composites	273	4.29	27

[a] T is the adsorption temperature, and n_e is the adsorption amount.

As listed in Table 2, the R^2 values of the F isotherms are closer to 1 than those of the L isotherms at the same temperature, and the mean deviations (ΔN) of the F isotherm are much less than that of the L isotherm. As shown in Figure 5, the F isotherm almost coincides with the experimental data; however, the L isotherm deviates from the experimental data, especially at high pressure. It indicates that the F equation is more suitable to describe the adsorption performance of H_2, CH_4, and CO_2 on HSAAC. The constant k and q in Table 2 are the F constants, and k can be regarded as the adsorption capacity of the adsorbent, which represents the gas quantity adsorbed over AC for a unit pressure, and q reflects the effect of pressure on the gas adsorption amount, giving an indication of the favorablity of the adsorption process. As listed in Table 2, both k and q increase with decreasing temperature, which exhibits a typical property of physical adsorption for CO_2 or CH_4 over the AC surface. The effective level of pressure on adsorption decreases, and the surface heterogeneity becomes more important in the range of low temperatures.[29] The relationship of k and q in the F equation with temperature can be described by the plot of ln k or $1/q$ vs T (Figure 6). Consequently, the adsorption amount of CO_2 [(226 to 301) K] and CH_4 [(176 to 213) K] in the pressure range of (0 to 101) kPa can be described by the following F equation:

$$n(CO_2) = kp^{1/q} = 5.5\cdot10^3 e^{-3.97\cdot10^{-2}T} p^{(-0.193+3.86\cdot10^{-3}T)} \quad (4)$$

$$n(CH_4) = kp^{1/q} = 7.4\cdot10^3 e^{-4.68\times10^{-2}T} p^{(-0.691+6.36\cdot10^{-3}T)} \quad (5)$$

According to eqs 4 and 5, we calculated the adsorption amount of CO_2[(226 to 301) K] and CH_4[(176 to 213) K] on corncob-derived AC and the prediction results are in good agreement with the experimental values over the pressure range of 20 to 100 kPa, as shown in Figure 7.

In addition, the Henry's law constant was used as a criterion for the adsorption affinity at low surface coverage and can be determined by the extrapolation of isothermal ln (p/n) versus n data to a zero adsorbed-phase concentration.[30] As listed in Table 3, the Henry's law constant of CO_2 on AC at 273 K was close to that observed on A10.[27] Furthermore, Henry's law constants for both CH_4 and CO_2 decreased with the increase of temperature,

Table 2. Parameters of the L and F Models for H_2, CH_4, and CO_2 at Different Temperatures

		Langmuir model				Freundlich model			
gas	T (K)	n_m (mmol·g^{-1})	b (kPa^{-1})	R^2	ΔN	K (mmol·g^{-1}· (kPa)$^{-1/q}$)	q	R^2	ΔN
H_2	77	11.502	0.103	0.972	0.108	1.664	2.186	0.990	0.044
CH_4	213	8.532	0.025	0.983	0.091	0.351	1.514	0.998	0.018
CH_4	195	9.451	0.052	0.978	0.074	0.782	1.807	0.996	0.029
CH_4	176	14.466	0.060	0.984	0.048	1.983	2.351	0.989	0.032
CO_2	301	5.287	0.008	0.961	0.151	0.038	1.051	0.986	0.062
CO_2	273	18.070	0.004	0.999	0.060	0.097	1.127	0.999	0.018
CO_2	226	20.773	0.019	0.994	0.043	0.728	1.495	0.998	0.017

which means that the adsorption capacity decreases with the increase in temperature, similar to that reported in the literature.[31]

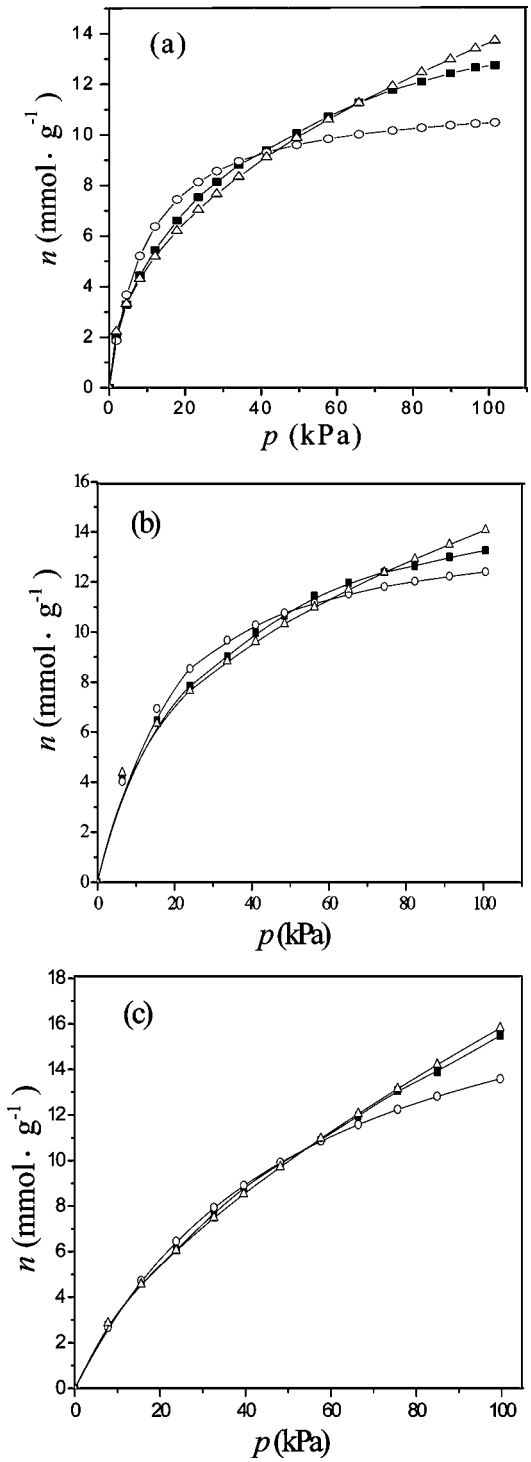

Figure 5. Equilibrium adsorption isotherms of (a) H_2 (77 K), (b) CH_4 (176 K), and (c) CO_2 (226 K): ■, experimental; ○, Langmuir; Δ, Freundlich.

The limiting heat of adsorption at zero coverage reflects the strength of the interaction between adsorbates and adsorbents,which can be calculated from the slopes of van't Hoff plots of Henry's law constants (K) against 1/T (Figure 8).[32] The limiting heat of CO_2 adsorption was 20.39 kJ·mol^{-1}, similar to that [(16.2 to 25.7) kJ·mol^{-1}] already reported in the literature whereas the limiting heat of CH_4 adsorption was 13.97 kJ·mol^{-1}, slightly lower than that [(16.1 to 20.6) kJ·mol^{-1}][31] observed over other materials due to the difference in temperature measured by us [(176 to 213) K] and by Himeno et al. [(273 to 333) K].[31]

If the adsorption was ideal, the adsorption heat should be independent of the adsorbate coverage. However, due to energetically heterogeneous surfaces over AC and the occurrence

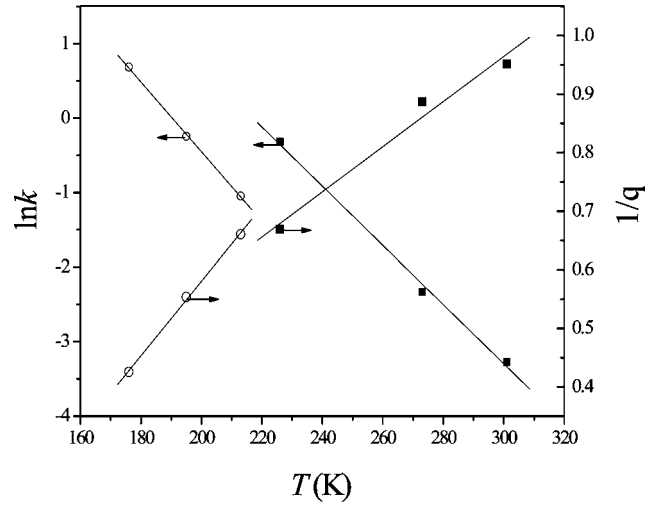

Figure 6. Plots of ln k or 1/q vs T for CH_4 (○) and CO_2 (■).

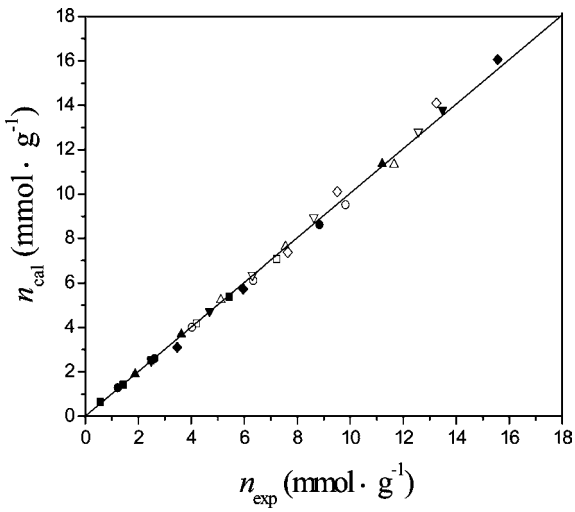

Figure 7. Calculated adsorption amounts n_{cal} vs experimental values n_{exp} for CH_4 (open symbol) and CO_2 (solid symbol): □, ■, 20 kPa; ○, ●, 40 kPa; △, ▲, 60 kPa; ▽, ▼, 80 kPa; ◇, ◆, 100 kPa.

Table 3. Henry's Law Constants for CH_4 and CO_2 Adsorption on AC

	K (CO_2)		K (CH_4)		
adsorbents	T (K)	(mol·kg^{-1}·kPa^{-1})	T (K)	(mol·kg^{-1}·kPa^{-1})	ref
AC	226	0.4640	176	1.177	this work
AC	273	0.0815	195	0.467	this work
AC	301	0.0299	213	0.224	this work
A10	273	0.0818			27
A10	298	0.0365			27

of interaction between adsorbates during gas adsorption, the heat of adsorption changes with different adsorption amounts. The isosteric enthalpy of adsorption is calculated by the Clausius−Clapeyron equation:[33]

$$\left[\frac{\partial \ln p}{\partial T}\right]_n = -\frac{\Delta H}{RT^2} \tag{6}$$

where ΔH is the isosteric enthalpy of adsorption. The isosteric enthalpies of adsorption were plotted as a function of the amount of gas adsorption, as shown in Figure 9. The isosteric enthalpies of CO_2 adsorption decreased slightly with increasing loading, indicating that the carbon surface is not energetically uniform and that the isosteric enthalpy of adsorption decreases due to the interaction of adsorbate with adsorbent. The isosteric

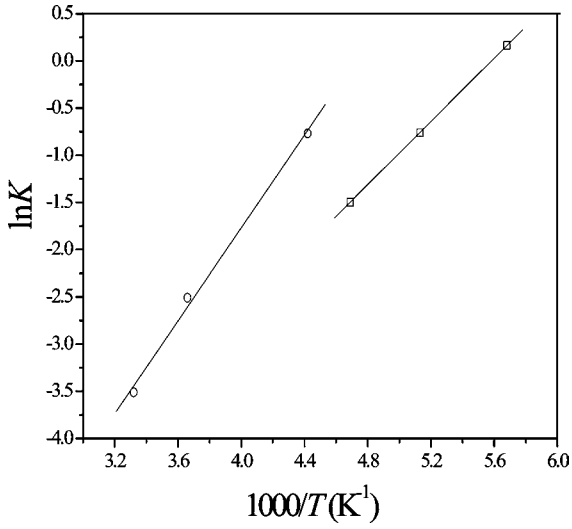

Figure 8. Van't Hoff plots of ln K vs 1/T: □, CH_4; ○, CO_2.

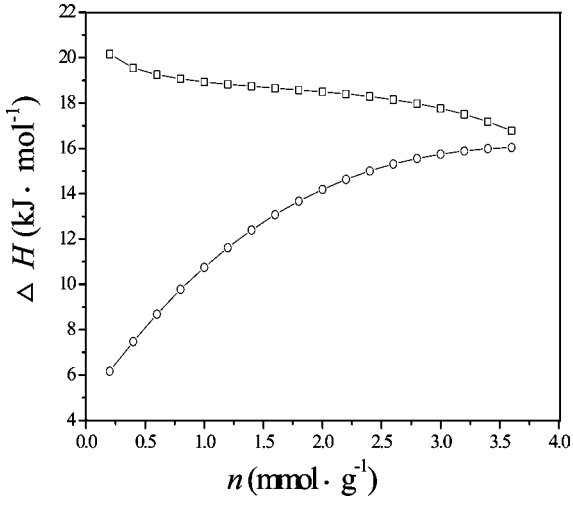

Figure 9. Variation of isosteric adsorption heat with amount adsorbed: □, CO_2; ○, CH_4.

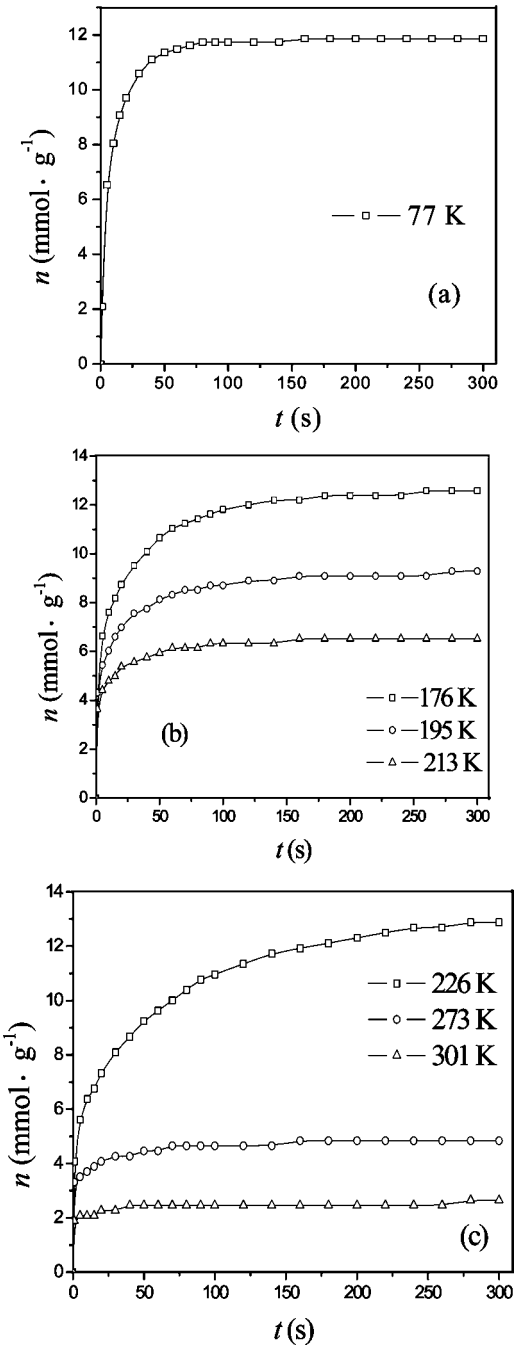

Figure 10. Relationship of adsorption amounts with time for (a) H_2, (b) CH_4, and (c) CO_2 at different temperatures.

enthalpies of CH_4 adsorption increase with the rise of the loading, indicating that the interaction between adsorbates is the main initial effect in the case of low methane coverage. The limiting adsorption heat of CO_2, determined by the extrapolation of the isosteric enthalpies of adsorption, was 20.65 kJ·mol^{-1}, in good agreement with that (20.39 kJ·mol^{-1}) determined by van't Hoff plots. However, the limiting adsorption heat of CH_4, determined by the extrapolation of the isosteric enthalpies of adsorption, was 4.95 kJ·mol^{-1}, lower than that (13.97 kJ·mol^{-1}) determined by the van't Hoff plots. The difference is attributed to the different calculation method and kinetic diameters of CH_4 (0.38 nm) and CO_2 (0.33 nm), as well as adsorption properties of CH_4 and CO_2 molecules at low temperature. The interaction between adsorbates affected CH_4 adsorption strongly at low coverage. It appeared that the limiting

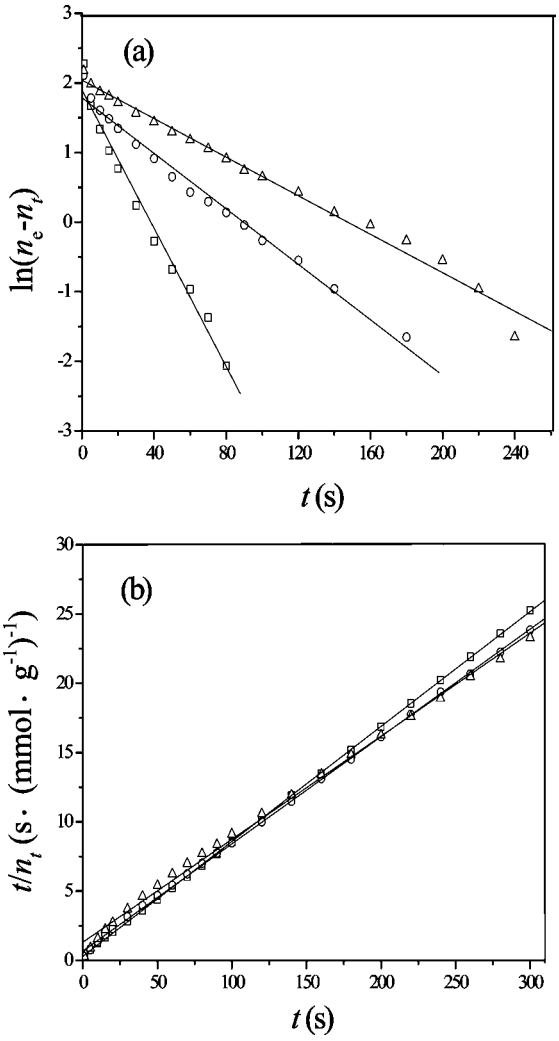

Figure 11. (a) Pseudo-first-order and (b) -second-order kinetics for H_2, CH_4, and CO_2: □, H_2 (77 K); ○, CH_4 (176 K); Δ, CO_2 (226 K).

adsorption heat was not properly determined by extrapolation of the isosteric adsorption enthalpies in such conditions.

Adsorption Kinetics of H_2, CH_4, and CO_2 onto Concorb-Derived AC. The variation of the adsorption amount with adsorption time at different temperatures is shown in Figure 10. The amount of the adsorbed gas increased with time at the initial stage of adsorption and became almost constant after ca. 100 s. At that time, the amount of gas adsorption and desorption over AC reached a dynamic equilibrium. The amount of gas adsorbed at the equilibrium time reflected the maximum adsorption capacity of the adsorbent under a given operational condition. These results indicate that the equilibrium adsorption capacities for CH_4 and CO_2 increases with decreasing temperature, and the lower adsorption temperature is, the longer the equilibrium time became due to slow thermal motion of gas molecules at low temperature.

Based on previous studies in adsorption kinetics, the adsorption behavior of plant-ACs are usually interpreted by the pseudo-first- and -second-order rate equations.[34,35] Any kinetic or mass transfer representation is likely to be global. In recent work, two kinetic models were adopted to illustrate the kinetics of corncob-based ACs. The integral equations of the pseudo-first- and -second-order models are expressed as:[34,36]

$$\ln(n_e - n_t) = \ln n_e - k_1 t \quad (7)$$

$$t/n_t = 1/(n_e^2 k_2) + t/n_e \quad (8)$$

where n_e and n_t are the adsorption amounts (mmol·g^{-1}) at equilibrium and at time t (s), respectively; k_1 (s^{-1}) and k_2 (g·mmol^{-1}·s^{-1}) are the rate constants for the pseudo-first- and -second-order model, respectively.

The rate constants of adsorption are determined from eq 7 and eq 8 (Figure 11), and the results are listed in Table 4. The rate constants k_1 and k_2 decrease with decreasing temperature, indicating that a longer time is required to reach equilibrium at lower temperature. The equilibrium adsorption amounts of CH_4 and CO_2 increase with decreasing temperature. The coefficients of determination of the second-order kinetics for H_2, CH_4, and CO_2 are greater than 0.996, and the experimental values ($n_{e,exp}$) agree well with the calculated ones ($n_{e,cal}$), indicating that performance of the adsorption procedure for CH_4 and CO_2 on AC can be described by the second-order kinetic equation. According to the Arrhenius formula:

$$k_2 = Ae^{-E_a/RT} \quad (9)$$

where R is the ideal gas constant, A is the frequency factor (g·mol^{-1}·s^{-1}), E_a is the activation energy (kJ·mol^{-1}), and T is absolute temperature (K). The activation energy for CH_4 and CO_2 adsorption on AC is (10.84 and 25.50) kJ·mol^{-1} (Figure 12), respectively. Therefore, the adsorption of CH_4 and CO_2 on AC exhibited physical adsorption based on a activation energy characteristic for physisorption [(5 to 40) kJ·mol^{-1}] and chemisorption [(40 to 800) kJ·mol^{-1}].[37]

Conclusions

Corncobs can be effectively used as a raw material for the preparation of HSAAC. The adsorption behavior of H_2, CH_4, and CO_2 at low temperature can be accurately described by the Freundlich equation. The maximum adsorption capacity of H_2, CH_4, and CO_2 on AC was (12.76 (77 K), 7.66 (213 K), and

Table 4. Comparison of Pseudo-First- and -Second-Order Adsorption Rate Constants and Calculated and Experimental n_e Values at Different Temperatures

			first-order kinetic model			second-order kinetic model		
gas	T (K)	$n_{e,exp}$ (mmol·g^{-1})	k_1 (s^{-1})	$n_{e,cal}$ (mmol·g^{-1})	R^2	k_2 (g·mmol^{-1}·s^{-1})	$n_{e,cal}$ (mmol·g^{-1})	R^2
H_2	77	11.86	0.050	6.686	0.981	0.022	12.06	0.999
CH_4	213	6.51	0.029	2.413	0.986	0.033	6.63	0.999
CH_4	195	9.28	0.021	3.783	0.980	0.016	9.39	0.999
CH_4	176	12.58	0.020	5.963	0.986	0.009	12.91	0.999
CO_2	301	2.65	0.034	0.734	0.989	0.112	2.56	0.997
CO_2	273	4.84	0.029	1.496	0.992	0.049	4.91	0.999
CO_2	226	12.88	0.014	7.693	0.988	0.004	13.44	0.996

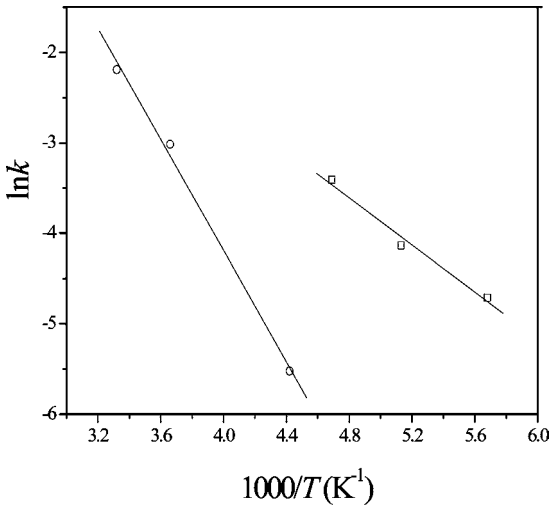

Figure 12. Arrhenius equation plots of ln k vs $1/T$: □, CH_4; ○, CO_2.

3.56 (301 K)) mmol·g^{-1}, respectively at 0.1 MPa, significantly higher than those reported in the literature. Kinetic data follow a pseudo-second-order kinetic model.

Literature Cited

(1) Tian, H. Y.; Buckley, C. E.; Wang, S. B.; Zhou, M. F. Enhanced hydrogen storage capacity in carbon aerogels treated with KOH. *Carbon* **2009**, *47*, 2128–2130.

(2) Radosz, M.; Hu, X. D.; Krutkramelis, K.; Shen, Y. Q. Flue-gas carbon capture on carbonaceous sorbents: toward a low-cost multifunctional carbon filter for "green" energy producers. *Ind. Eng. Chem. Res.* **2008**, *47*, 3783–3794.

(3) Ruthven, D. M. *Principles of adsorption and adsorption processes*; John Wiley & Sons: New York, 1984.

(4) El-Hendawy, A. A.; Samra, S. E.; Girgis, B. S. Adsorption characteristics of activated carbons obtained from corncobs. *Colloids Surf., A* **2001**, *180*, 209–221.

(5) El-Hendawy, A. A. Surface and adsorptive properties of carbons prepared from biomass. *Appl. Surf. Sci.* **2005**, *252*, 287–295.

(6) El-Hendawy, A. A. Influence of HNO_3 oxidation on the structure and adsorptive properties of corncob-based activated carbon. *Carbon* **2003**, *41*, 713–722.

(7) Aworn, A.; Thiravetyan, P.; Nakbanpote, W. Preparation and characteristics of agricultural waste activated carbon by physical activation having micro- and mesopores. *J. Anal. Appl. Pyrolysis* **2008**, *82*, 279–285.

(8) Aworn, A.; Thiravetyan, P.; Nakbanpote, W. Preparation of CO_2 activated carbon from corncob for monoethylene glycol adsorption. *Colloids Surf., A* **2009**, *333*, 19–25.

(9) Cao, Q.; Xie, K. C.; Lv, Y. K.; Bao, W. R. Process effects on activated carbon with large specific surface area from corncob. *Bioresour. Technol.* **2006**, *97*, 110–115.

(10) Tseng, R. L.; Tseng, S. K. Pore structure and adsorption performance of the KOH-activated carbons prepared from corncob. *J. Colloid Interface Sci.* **2005**, *287*, 428–437.

(11) Tseng, R. L.; Tseng, S. K.; Wu, F. C. Preparation of high surface area carbons from corncob with KOH etching plus CO_2 gasification for the adsorption of dyes and phenols from water. *Colloids Surf., A* **2006**, *279*, 69–78.

(12) Su, W.; Zhou, L.; Zhou, Y. P. Preparation of microporous activated carbon from coconut shells without activating agents. *Carbon* **2003**, *41*, 861–863.

(13) Brunauer, S.; Emmett, P. H.; Teller, E. Adsorption of gases in multimolecular layers. *J. Am. Chem. Soc.* **1938**, *60*, 309–319.

(14) Rangarajan, B.; Lira, C. T.; Subramanian, R. Simplified local density model for adsorption over large pressure ranges. *AIChE J.* **1995**, *41*, 838–845.

(15) Cazorla-Amorós, D.; Alcañiz-Monge, J.; Linares-Solano, A. Characterization of activated carbon fibers by CO_2 adsorption. *Langmuir* **1996**, *12*, 2820–2824.

(16) Nijkamp, M. G.; Raaymakers, J. E. M. J.; Dillen, A. J.; Jong, K. P. Hydrogen storage using physisorption-materials demands. *Appl. Phys. A: Mater. Sci. Process.* **2001**, *72*, 619–623.

(17) Yang, S. J.; Cho, J. H.; Oh, G. H.; Nahm, K. S.; Park, C. R. Easy synthesis of highly nitrogen-enriched graphitic carbon with a high hydrogen storage capacity at room temperature. *Carbon* **2009**, *47*, 1585–1591.

(18) Panella, B.; Hirscher, M.; Pütter, H.; Müller, U. Hydrogen adsorption in metal-organic frameworks: Cu-MOFs and Zn-MOFs compared. *Adv. Funct. Mater.* **2006**, *16*, 520–524.

(19) Panella, B.; Hirscher, M.; Roth, S. Hydrogen adsorption in different carbon nanostructures. *Carbon* **2005**, *43*, 2209–2214.

(20) Vasiliev, L. L.; Kanonchik, L. E.; Kulakov, A. G.; Mishkinis, D. A.; Safonova, A. M.; Luneva, N. K. New sorbent materials for the hydrogen storage and transportation. *Int. J. Hydrogen Energy* **2007**, *32*, 5015–5025.

(21) Lee, S. M.; Park, S. H.; Lee, S. C.; Kim, H. J. Adsorption properties of N_2, H_2 on single-walled carbon nanotubes modified by KOH. *Chem. Phys. Lett.* **2006**, *432*, 518–522.

(22) Pevida, C.; Drage, T. C.; Snape, C. E. Silica-templated melamine-formaldehyde resin derived adsorbents for CO_2 capture. *Carbon* **2008**, *46*, 1464–1474.

(23) Pevida, C.; Plaza, M. G.; Arias, B.; Fermoso, J.; Rubiera, F.; Pis, J. J. Surface modification of activated carbons for CO_2 capture. *Appl. Surf. Sci.* **2008**, *254*, 7165–7172.

(24) Plaza, M. G.; Pevida, C.; Arenillas, A.; Rubiera, F.; Pis, J. J. CO_2 capture by adsorption with nitrogen enriched carbons. *Fuel* **2007**, *86*, 2204–2212.

(25) Maroto-Valer, M. M.; Tang, Z.; Zhang, Y. Z. CO_2 capture by activated and impregnated anthracites. *Fuel Process. Technol.* **2005**, *86*, 1487–1502.

(26) Hernández-Huesca, R.; Díaz, L.; Aguilar-Armenta, G. Adsorption equilibria and kinetics of CO_2, CH_4 and N_2 in natural zeolites. *Sep. Purif. Technol.* **1999**, *15*, 163–173.

(27) An, H.; Feng, B.; Su, S. CO_2 capture capacities of activated carbon fibre-phenolic resin composites. *Carbon* **2009**, *47*, 2396–2405.

(28) Weber, W. J., Jr. *Physico-chemical processes for water quality control*; Wiley Interscience: New York, 1972.

(29) Haghseresht, F.; Lu, G. Q. Adsorption characteristics of phenolic compounds onto coal-reject-derived adsorbents. *Energy Fuels* **1998**, *12*, 1100–1107.

(30) Zhang, S. Y.; Talu, O.; Hayhurst, D. T. High-pressure adsorption of methane in zeolites NaX, MgX, CaX, SrX and BaX. *J. Phys. Chem.* **1991**, *95*, 1722–1726.

(31) Himeno, S.; Komatsu, T.; Fujita, S. High-pressure adsorption equilibria of methane and carbon dioxide on several activated carbons. *J. Chem. Eng. Data* **2005**, *50*, 369–376.

(32) Sun, M. S.; Shah, D. B.; Xu, H. H.; Talu, O. Adsorption equilibria of C_1 to C_4 alkanes, CO_2, and SF_6 on silicalite. *J. Phys. Chem. B* **1998**, *102*, 1466–1473.

(33) Young, D. M.; Crowell, A. D. *Physical adsorption of gases*; Butterworths: London, 1962.

(34) Rajoriya, R. K.; Prasad, B.; Mishra, I. M.; Wasewar, K. L. Adsorption of benzaldehyde on granular activated carbon: kinetics, equilibrium, and thermodynamic. *Chem. Biochem. Eng. Q.* **2007**, *21*, 219–226.

(35) Hameed, B. H.; Din, A. T. M.; Ahmad, A. L. Adsorption of methylene blue onto bamboo-based activated carbon: Kinetics and equilibrium studies. *J. Hazard. Mater.* **2007**, *141*, 819–825.

(36) Ho, Y. S.; McKay, G. Sorption of dye from aqueous solution by peat. *Chem. Eng. J.* **1998**, *70*, 115–124.

(37) Banerjee, K.; Cheremisinoff, P. N.; Cheng, S. L. Adsorption kinetics of o-xylene by fly ash. *Water Res.* **1997**, *31*, 249–261.

Received for review March 25, 2010. Accepted August 28, 2010.

JE1002913